PRE-CLINICAL EVALUATION OF A NEW CORAL-BASED BONE SCAFFOLD

F. CARINCI[1], A. SANTARELLI[2], L. LAINO[3], F. PEZZETTI[4], A. DE LILLO[3], D. PARISI[3], F. BAMBINI[2], M. PROCACCINI[2], N.F. TESTA[5], R. COCCHI[6] and L. LO MUZIO[3]

[1]Department of Experimental Morphology, Surgery and Medicine, Ferrara University, Ferrara, Italy; [2]Department of Clinic Specialistic and Stomatological Sciences, Marche Polytechnic University, Ancona, Italy; [3]Department of Clinical and Experimental Medicine, Foggia University, Foggia, Italy; [4]Department of Specialistic, Diagnostic and Experimental Medicine, Bologna University, Bologna, Italy; [5]Interdisciplinary Department of Medicine, Bari University, Bari, Italy; [6]IRCCS Casa Sollievo della Sofferenza, S. Giovanni Rotondo, Foggia, Italy

Received September 11, 2013 – Accepted March 12, 2014

Coral is used worldwide for bone reconstruction. The favorable characteristics that make this material desirable for implantation are (i) osteoinduction, (ii) and osteoconduction. These proprieties have been demonstrated by *in vivo* studies with animal models and clinical trials over a twenty-year period. Also poly(2-hydroxyethylmethacrylate) [poly(HEMA)] is a widely used biomaterial. By using coral and poly(HEMA), a scaffold for bone reconstruction application has been recently synthesized. Cytological, histological and genetic analyses were performed to characterize this new alloplastic material. Four samples were analyzed: (a) white coral (WC), (b) red coral (RC), (c) WC plus polymer (WCP) and (d) RC plus polymer (RCP). Quantification of mitochondrial dehydrogenase activity by MTT assay was performed as indirect detector of cytotoxicity. *In vivo* effects were revealed by implanting corals and coral-based polymers in rabbit tibia. Samples were collected after 4 weeks and subjected to histological analysis. To evaluate the genetic response of cells to corals and coral-derived polymers an osteoblast-like cell line (i.e. MG63) was cultured in wells containing (a) medium, (b) medium plus corals and (c) medium plus two types of scaffolds (RCP or WCP). RNAs extracted from cells were retro-transcribed and hybridized on DNA 19.2K microarrays. No cytotoxicity was detected in corals and coral-based biopolymers. No inflammation or adverse effect was revealed by histological examination. By microarray analysis 154 clones were differentially expressed between RC and WC (81 up and 73 down regulated) whereas only 15 clones were repressed by the polymer. Histological evaluation not only confirmed that coral is a biocompatible material, but also that the polymer has no adverse effect. Microarray results were in agreement with cytological and histological analyses and provided further data regarding the genetic effects of RC, WC and the new polymer.

The coral or *Madreporaria* skeleton is morphologically and chemically close to mineral bone. It is a cheap, natural biomaterial with excellent biocompatibility. Coral can easily be shaped and it has been successfully used as a bone substitute in the clinical practice since the eighties (1) to treat patients affected by craniofacial syndromes (2), as a replacement graft material in periodontal bone loss

Key words: bone, coral, scaffold, polymer, cDNA microarray

Mailing address:
Prof. Lorenzo Lo Muzio,
Via Rovelli, 48
71122 Foggia, Italy
Tel.: +39 0881 588090
Fax: +39 0881 588081
e-mail: lorenzo.lomuzio@unifg.it

0394-6320 (2014)

DISCLOSURE: ALL AUTHORS REPORT NO CONFLICTS OF INTEREST RELEVANT TO THIS ARTICLE.

(3), and in post-traumatic dento-alveolar defects (4).

Coral is composed mainly of calcium carbonate in the form of aragonite (97-98%). It has a porosity of more than 45%, with pores of about 150 μm diameter. The coral is degradable and the degradation appears to be related to the amount of porosity of the coral (5) and it may take two forms (6): dissolution at the surface, or resorption by macrophages and multinucleated giant cells. The degradation of coral has been reported to be species specific: a 100% degradation in a 3-month period has been reported in a rabbit tibia model (7). Coral, moreover, has a potential to improve bone regeneration, does not evoke an inflammatory infiltrate or a fibrous encapsulation (8).

The red coral *Corallium rubrum* has two types of skeletal structures: an axial skeleton and microscopic, and calcareous spicules that form a fragmented skeleton distributed through the mesoglea (9). The white corals *Madrepora oculata* and *Lophelia pertusa* are of the *Scleractinia* type. Their skeletons are made from calcium carbonate in the form of aragonite, and develop from the basal disc of the polyp, growing outward (10).

Poly(2-hydroxyethylmethacrylate) [poly(HEMA)] is a widely-used biomaterial, due to its attractive features, like non-toxicity, favorable tissue compatibility and mechanical properties similar to those of natural tissue (11). It has been extensively used alone or as a carrier for several medical applications such as in the ophthalmologic field (12) or as a drug delivery vehicle (13). Another field for application of poly(HEMA) is engineered scaffolds for several tissues, such as heart muscle tissue (14) or bone (15).

Recently, a poly(HEMA) polymer was synthesized (16, 17). Because it can include coral, two types of biopolymers were obtained: WC plus polymer (WCP) and RC plus polymer (RCP).

In the present study the biological proprieties of RC, WC, RCP and WCP are investigated from cytological, histological and genetic points of view to obtain information regarding corals and poly(HEMA) polymer biocompatibility.

MATERIALS AND METHODS

Chemicals and corals

2-hydroxyethyl methacrylate (HEMA), methyl methacrylate (MMA) and 2,2' azoisobutyronitrile (AIBN) were supplied by FLUKA, Milan, Italy. All reagents for cell cultures were obtained from Hyclone, Milan, Italy. Plastic tissue cultures were from Falcon, Milan, Italy. WC was supplied by B.&B. Dental s.r.l. Bologna, Italy. RC granules from *Porites sp.* consist of calcium carbonate (98-99%) in the form of aragonite, trace elements (0.5-1%) and amino acids (0.07±0.02%). RC granules were sterilized by autoclaving. Coral composition was not affected by autoclaving.

Polymer synthesis

A 50/50 wt% mix of 2-hydroxyethyl methacrylate and methyl methacrylate (HEMA-co-MMA) was prepared with 0.1% w/w of 2-2'-azoisobutyrronitrile (AIBN) as initiator. Preliminary studies showed this ratio to have the appropriate viscosity to suspend the coral particles with only minimal sedimentation. RC and WC were added at 30 wt% of HEMA-co-MMA solution, stirred under magnetism for 3 h at 70°C. The scaffolds were sectioned into 2-mm thick disks using a slow speed diamond saw. Prior to the swelling experiments the disks were washed extensively with double-distilled water to eliminate all unpolymerized monomer. Differential Scanning Calorimeter (DSC) was employed to optimize the polymerization thermal conditions and to evaluate the Glass Transition of synthesized materials. The tests were carried out by using a DuPont calorimeter under nitrogen flow.

Sample preparation

All disks were scrubbed under running tap water to remove gross debris. The disks were then placed in double-distilled water and ultrasonically cleaned for 15 min. The samples were then placed in a 1% solution of Liquinox, placed in an ultrasound sonicator for 15 min followed by a final 15 min ultrasonic rinse with double-distilled water. All disks were then sterilized in UV light for 20 min per side.

Cytotoxic assay

Detection of cytotoxicity effects was performed indirectly by quantification of mitochondrial dehydrogenase activity by MTT assay (Sigma, Milan, Italy). MTT is the abbreviated notation for tetrazolium salt [3-(4,5-dimethylthiazol-2-yl)-2,5-diphenyl tetrazolium bromide]. Tetrazolium salts are used extensively in cell proliferation and cytotoxicity assays; in particular, MTT colorimetric assay is accepted as a routine cytotoxicity test and can be useful for preliminary screening for toxicity of biomaterials. This salt is initially colorless and is metabolically reduced to highly colored end products called formazans by the activity of living cells. Most cellular bioreduction of MTT is associated with enzymes of the endoplasmic reticulum: the MTT

enters the cells and passes into the mitochondria where the tetrazolium ring in MTT is cleaved by dehydrogenases present in active mitochondria, resulting in the formation of an insoluble, colored, formazan product. The cells are then solubilized with an organic solvent (isopropanol) and the released, solubilized formazan reagent is measured spectrophotometrically (λ =570 nm). Since reduction of MTT can only occur in metabolically active cells, the level of activity is a measure of the viability of the cells. The percentage of the dehydrogenase activity was calculated from the absorbance values and compared with that of the control. The assay was performed using human lymphoblastoid cell lines (CCL-86, ATCC, Rockville, MD) in 24-well tissue culture plates for 24 and 48 h. Tissue culture polystyrene (TCPS) was used as a positive control. The original medium was replaced by 1 ml of DMEM without phenol red and 0.1 ml of MTT solution (5 mg/ml in DMEM without phenol red) and the culture plate was returned to the incubator for 2-4 h. After the incubation period, 1 mL of MTT solubilization solution (10% Triton X-100 plus 0.1N HCl in anhydrous isopropanol) was added to each well and mixed thoroughly, releasing the blue formazan crystals. The samples were left on a rotating plate for 1 h. After formation of formazan crystals, the culture medium supernatant was removed from the wells without disruption of the formazan precipitate. The absorbance was read at wavelength of 570 nm using a spectrophotometer. Three independent growth experiments were undertaken for each tested material.

Animal model

Seven New Zealand rabbits were used in the study, upon approval of the Ethics Committee for Human and Animal studies of the School of Medicine, University of Chieti, Italy. The rabbits, weighing approximately 2.5 kg, were kept in cages in the same institution. Each rabbit was sedated with midazolam (2 mg/kg IM) before placement of an intravenous (IV) catheter in the marginal ear vein. The animals were anaesthetized with a dose of Ketamine (Ketalar, Parke-Davis S.p.A., Milan, Italy) and xylazine (Rompum, Bayer AG, Leverkusen, Germany). The ketamine was used to the dose of 44 mg/Kg and the xylazine to the dose of 6-8 mg/Kg per kilo of weight. A local injection of 1.8 ml of Lidocaine without vasoconstrictor was performed (Lidocaine, Astra, Sodertalje, Sweden). A full thickness incision was performed to expose the upper anterior portion of the tibia. Two 6 mm bone defects were created in each tibia. Six defects were filled with WC, 6 defects were filled with RC, 6 defects were filled with WCP, 6 defects were filled with RCP and 4 defects were used as a control group. A total of 28 defects were created. The surgical wounds were sutured with stainless steel monofilament Wire 3.0 (Ethicon, J & J Somerville, New Jersey, USA). After the surgical procedures a single dose of antibiotic was administered (0.25 gr, Cefazolin IM). The post-operative course was uneventful. All rabbits were sacrificed with an overdose of Tanax T-61 after 4 weeks. All 28 defects were recovered. The area of interest in the tibia was exposed and a block section was retrieved by means of a Stryker Oscillating Orthopedic saw (Scientific Equipment Liquidators, Big Lake, MN USA). The specimens were immediately fixed in 10% formalin and processed to obtain thin ground sections with the Precise 1 Automated System (Assing, Rome, Italy). For each specimen, three slides were obtained and stained with acid fuchsine and toluidine blue. The slides were examined by an independent examiner in normal transmitted light under a Leitz Laborlux microscope (Leitz, Wetzlar, Germany). Histomorphometry of the new bone percentage and residual biomaterials was carried out using a light microscope connected to a high-resolution video camera (3CCD, JVC KY-F55B) and interfaced to a monitor and PC (Intel Pentium IV 3000 MMX). This optical system was associated with a digitizing pad (Matrix Vision GmbH) and a histometry software package with image capturing capabilities.

Statistical evaluation

The differences in the percentage of newly-formed bone and residual grafted in the different Groups were evaluated with the Analysis of Variance (ANOVA). The significance of the differences observed was evaluated with Bonferroni test for multiple comparisons. The percentages were expressed as a mean +/- standard deviation and standard error. Statistically significant differences were set at $p<0.05$. All the data were analyzed by means of the computerized statistical package Primer 4.02 (McGraw Hill Inc., New York, USA).

Cell line

Osteoblast-like cell (MG63, ATCC, Rockville, MD) were cultured in sterile Falcon wells using Eagle's minimum essential medium (MEM) supplemented with 10% fetal calf serum (FCS) (Sigma, Chemical Co., St Louis, Mo, USA). Cultures were maintained in a 5% CO_2 humidified atmosphere at 37°C.

MG63 cells were collected and seeded at a density of $1x10^5$ cells/ml into 9 cm^2 (3 ml) wells containing of 3 ml of MEM with 10% FCS. Sets of wells contained different sterile samples: (1) WC (10 mg/ml), (2) RC (10 mg/ml), (3) WCP (10 mg/ml) and (4) RCP (10 mg/ml). Additional sets had only medium and cells. After 24 h the cells from all wells were processed for RNA extraction.

Microarray analysis

RNA was extracted by using RNAzol. Ten micrograms of total RNA were used for each sample. cDNA was

synthesized by using Superscript II (Life Technologies, Invitrogen, Milano, Italy) and amino-allyl dUTP (Sigma). Mono-reactive Cy3 and Cy5 esters (Amersham Pharmacia, Little Chalfont, UK) were used for indirect cDNA labelling. RNA extracted from untreated MG63 was labeled with Cy3 and used as control against the Cy5 labeled treated MG63 (i.e. WC, RC, WCP and RCP) cDNA in the first experiment and then switched. Human 19.2 K DNA microarrays were used (Ontario Cancer Institute, Toronto, Canada). For 19.2 K slides 100 μL of the sample and control cDNAs in DIG Easy hybridization solution (Roche, Basel, Switzerland) were used in a sandwich hybridization of the two slides constituting the 19.2 K set at 37°C overnight. Washing was performed three times for 10 min with 1x saline sodium citrate (SSC), 0.1% sodium dodecyl sulphate (SDS) at 42°C, and three times for 5 min with 0.1 x SSC at room temperature. Slides were dried by centrifugation for 2 min at 2000 rpm. The experiment was repeated twice and the dyes switched. A GenePix 4000a DNA microarrays scanner (Axon, Union City, CA, USA) was used to scan the slides, and data were extracted with GenePix Pro. Genes with expression levels, after removing local background, of less than 1000 were not included in the analysis, since ratios are not reliable at that detection level (18-20).

After scanning the two slides containing the 19,200 human genes in duplicate, local background was calculated for each target location. A normalization factor was estimated from ratios of median. Normalization was performed, by adding the $\log_2$ of the normalization factor to the $\log_2$ of the ratio of medians. The $\log_2$ ratios for all the targets on the array were then calibrated using the normalization factor, and $\log_2$ ratios outside the 99.7% confidence interval (the median +/-3 times the SD = 0.52) were determined as significantly changed in the treated cells. Thus genes are significantly modulated in expression when the absolute value of their $\log_2$ expression level is higher than 1.56, or else there is a 3-fold difference in expression between treated cells and reference. GenePix Pro software was used to report genes above the threshold and with less than 10% difference in three different statistical evaluations of the intensity ratio, thus effectively enabling an automated quality control check of the hybridized spots. Furthermore, all the positively passed spots were finally inspected visually. SAM (significance analysis of microarray) program was then carried out and SAM score was obtained (T-statistic value) (18).

RESULTS

Cytotoxic assay

Lymphoblastoid cell line was used for direct contact test at 24 h and 48 h. Proliferation and cell viability were determined by MTT test. The results were obtained referring the absorbance values at 570 nm ($O.D._{570}$) of cell exposed to materials with that of control. Cell number and viability were determined using Trypan blue exclusion test. Our results show that the polymers supported the proliferation and growth of cells and did not elicit any evident cytotoxic effect (Fig. 1).

Microscopical features of animal specimens

Control - A limited quantity of newly formed bone was present in the cortical portion, and the marrow defects had not been filled by the regenerated bone.

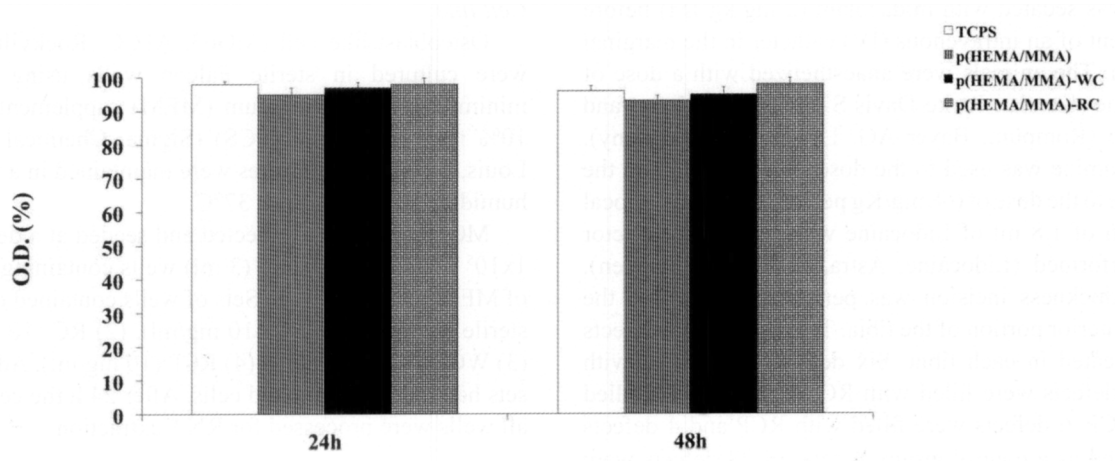

Fig. 1. *Cytotoxic assay of lymphoblastoid cell line at direct contact with biomaterials at 24 h and 48 h.*

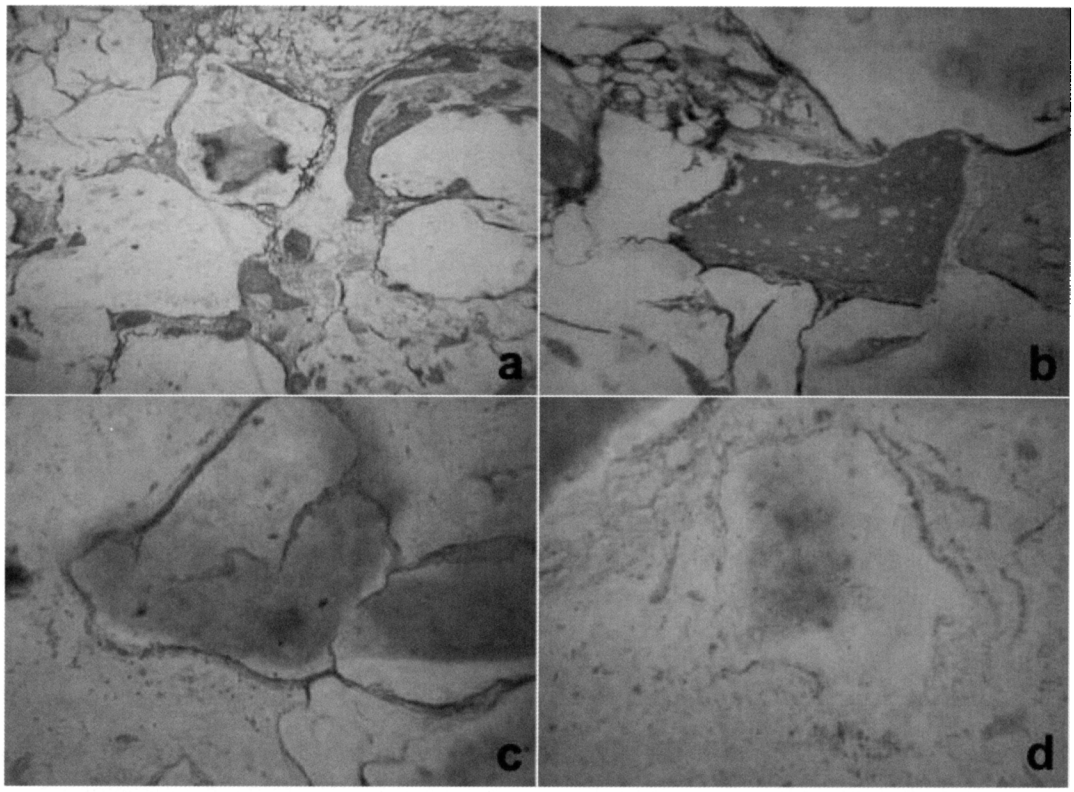

Fig. 2. ***a)*** *New osteogenesis is present between WC particles (Acid fuchsin and toluidine blue, original magnification 18X).* ***b)*** *Most of the particles of WCP are surrounded by new bone. No multinucleated cells similar to osteoclasts are present (Acid fuchsin and toluidine blue, original magnification 50X).* ***c)*** *RC is colonised with fluid and cells (Acid fuchsin and toluidine blue, magnification 50X).* ***d)*** *A particles of RCP is completely colonised by cells and biological fluid (Acid fuchsin and toluidine blue, original magnification 50X).*

The newly-formed bone was intensively stained with acid fuchsine and presented large osteocytic lacunae. At higher magnification, many actively secreting osteoblasts were observed at the periphery of the bone defects. No trabecular bone or osteoblasts were present in the central portion of the defects. The rest of the bone cavity contained fibrous tissue with a few inflammatory cells. The inflammatory reaction was characterized by foci of lymphocytes distributed around the periphery of the cavity. No multinucleated cells were observed. Histomorphometry showed that the percentage of newly formed bone was 4±0.5%.

WC - Most of the WC particles were found within the newly formed bone and were almost completely surrounded by lamellar and trabecular mature bone. It was possible to observe the formation of a small quantity of bone only around a few particles found in the marrow space. The bone was in direct contact with the particles of the biomaterial, and no gaps were present between WC and bone. Neither inflammatory cell infiltrate nor multinucleated cells were present around the particles of the biomaterial. Histomorphometry showed that the percentage of newly formed bone was 22±2%, and residual WC was 34±2.6.

WCP - No acute inflammatory cell infiltrate was present. Most of the particles found in the regenerated bone appeared to be in the process of undergoing resorption in the periphery of the particle. Most of the particles were surrounded by a space filled by multinucleated cells similar to osteoclasts. No trabecular bone was present in the central portion of the defects. Histomorphometry showed that the percentage of newly formed bone was 24±1.6% while the residual WC was 21±2.6.

RC – Microscopically, it was possible to see newly formed bone with the presence of large osteocyte lacunae, while lamellar bone and Haversian system

Table I. *Histomorphometry of percentage of newly formed bone and residual grafted materials.*

	Percentage of newly formed bone	Percentage of residual grafted materials
Control	4±0.5	
WC	22±2	34±2.6
WCP	24±1.6	21±2.6
RC	25±1.2	36±3.6
RCP	27±3.2	23±4.6

were not present. New bone surrounded the RC. Inflammatory and multinucleated cells were absent in all specimens. Some small osteoblasts were observed near the RC. The biomaterial was colonized with fluids and cells. Histomorphometry showed that the percentage of newly formed bone was 25±1.2%, and the residual RC was 36±3.6.

RCP - Newly formed trabecular bone was observed in the external portion of the bone defects, whereas no bone was present in the central area of the defects. The newly formed bone was stained more intensively than the pre-existing bone with acid fuchsine. Multinucleated cells and lymphoplasmacells were present only in a few areas. Osteoblasts secreting bone were observed near the RCP. Histomorphometry showed that the percentage of newly formed bone was 27±3.2%, while the residual WC was 23±4.6.

Statistical evaluation

Statistically significant differences were found in the percentage of newly formed bone between WC, WCP, RC, RCP and control specimens. Indeed, the amount of newly formed bone was greater in samples with biomaterial in respect to control ones, regardless the type of biomaterial ($p<0.05$). Statistically significant differences were found in the percentage of residual grafted materials between the different WC, RC and WCP and RCP. Indeed, when the polymer was added, specimens displayed less residual graft material, regardless of whether white or red coral was employed (Table I).

Microarray analysis

The genes differentially expressed between (i) corals *vs* untreated MG63, (ii) RC *vs* WC and (iii) RC+WC *vs* RCP+WCP are reported in Tables II, III and IV, respectively.

Hybridization of mRNA-derived probes to cDNA microarrays allowed us to perform systemic analysis of expression profiles for thousands of genes simultaneously and to provide primary information on transcriptional changes related to the effect of (1) corals on osteoblast-like cells, (2) type of coral and (3) presence/absence of polymer.

Effect of corals on osteoblast-like cells

Very few genes are up-regulated and none has a major regulatory role. Among the down-regulated genes some are involved in signal transduction [such as: OPHN1 (oligophrenin 1), a Rho-GTPase-activating protein; GREB1 (growth regulation by estrogen in breast cancer 1), an estrogen-responsive gene; and RXRB (retinoid x receptor beta), a receptor that forms homodimers with the retinoic acid, thyroid hormone, and vitamin D receptors, increasing both DNA binding and transcriptional function on their respective response elements], immune response [such as: CSF1 (colony stimulating factor 1), a cytokine that controls the production, differentiation, and function of macrophages; BAT1 (HLA-B associated transcript 1), a negative regulator of inflammation; SCYE1 (small inducible cytokine subfamily E member 1), a cytokine that is specifically induced by apoptosis; and LTBR (lymphotoxin beta receptor), a protein that plays a role in the development and organization of lymphoid tissue] and apoptosis [such as IGF1R (insulin-like growth factor 1 receptor), an anti-apoptotic agent)]. Additional notable genes are those of extracellular matrix components such as COL1A2 (collagen type 1 alpha 2) that encodes one of the chains for type I collagen, the fibrillar collagen found in most connective tissues and that has a role in osteogenesis, as well as CD44, a receptor for several ligands like hyaluronic acid, osteopontin, collagens, and matrix metalloproteinases (Table III).

Effect of coral type

Notable genes overexpressed in RC are those

Table II. *A) 2 up-regulated genes with known function selected from 6 clones obtained by microarray analysis from MG63 cultured with RC and WC vs MG63 cultured without corals.*

Name	Symbol	UGCluster	Score(d)
coiled-coil-helix-coiled-coil-helix domain containing 7	CHCHD7	Hs.436913	0.990579803
ferritin, light polypeptide	FTL	Hs.433670	0.887407277

B) 56 down-regulated genes with known function selected from 120 clones obtained by microarray analysis from MG63 cultured with RC and WC vs MG63 cultured without corals

Name	Symbol	UGCluster	Score(d)
actin, gamma 2, smooth muscle, enteric	ACTG2	Hs.403989	-1.152723912
alpha-1-B glycoprotein	A1BG	Hs.390608	-1.008167721
ethylmalonic encephalopathy 1	ETHE1	Hs.7486	-0.964040029
oligophrenin 1	OPHN1	Hs.128824	-0.934903792
ribosomal protein S29	RPS29	Hs.539	-0.910802193
UDP-Gal:betaGlcNAc beta 1,3-galactosyltransferase, polypeptide 4	B3GALT4	Hs.275865	-0.908565004
chromosome 14 open reading frame 45	C14orf45	Hs.260555	-0.888081725
colony stimulating factor 1 (macrophage)	CSF1	Hs.173894	-0.876799447
lymphotoxin beta receptor (TNFR superfamily, member 3)	LTBR	Hs.1116	-0.868653947
pregnancy specific beta-1-glycoprotein 1	PSG1	Hs.446644	-0.859219983
ubiquitin specific protease 37	USP37	Hs.166068	-0.852933798
zinc finger protein 307	ZNF307	Hs.44720	-0.845165108
S-adenosylhomocysteine hydrolase-like 1	AHCYL1	Hs.4113	-0.844715429
HLA-B associated transcript 1	BAT1	Hs.254042	-0.813601439
S100 calcium binding protein A11 (calgizzarin)	S100A11	Hs.417004	-0.806270942
serine/threonine kinase with Dbl- and pleckstrin homology domains	TRAD	Hs.162189	-0.805094448
tubulin, beta, 4	TUBB4	Hs.511743	-0.786363857
lysosomal-associated membrane protein 1	LAMP1	Hs.150101	-0.78029714
cofilin 1 (non-muscle)	CFL1	Hs.170622	-0.774259963
glycophorin E	GYPE	Hs.395535	-0.773867826
IKK interacting protein	IKIP	Hs.406199	-0.769993736
up-regulated in liver cancer 1	UPLC1	Hs.437379	-0.758647001
ribosomal protein, large, P1	RPLP1	Hs.356502	-0.757449376
cytochrome P450, family 2, subfamily D, polypeptide 6	CYP2D6	Hs.333497	-0.746704464
small inducible cytokine subfamily E, member 1 (endothelial monocyte-activating)	SCYE1	Hs.105656	-0.730297034
stromal cell protein	LOC55974	Hs.292154	-0.724004304
ribosomal protein L37a	RPL37A	Hs.433701	-0.718286276
ribosomal protein S3A	RPS3A	Hs.356572	-0.716907092
cholinergic receptor, nicotinic, alpha polypeptide 5	CHRNA5	Hs.1614	-0.708457315
prothymosin, alpha (gene sequence 28)	PTMA	Hs.459927	-0.708411941
ribosomal protein L13a	RPL13A	Hs.449070	-0.708008835

pregnancy specific beta-1-glycoprotein 6	PSG6	Hs.512646	-0.707675747
translocated promoter region (to activated MET oncogene)	TPR	Hs.170472	-0.704063541
hypothetical protein MGC5178	MGC5178	Hs.458369	-0.684077809
collagen, type I, alpha 2	COL1A2	Hs.232115	-0.678088475
RUN and TBC1 domain containing 2	RUTBC2	Hs.413265	-0.676579124
insulin-like growth factor 1 receptor	IGF1R	Hs.239176	-0.673826861
immunoglobulin lambda joining 3	IGLJ3	Hs.449601	-0.670285745
olfactomedin 1	OLFM1	Hs.74376	-0.667812154
GREB1 protein	GREB1	Hs.438037	-0.663411295
glyceraldehyde-3-phosphate dehydrogenase	GAPD	Hs.169476	-0.661394337
ribosomal protein S3A	RPS3A	Hs.356572	-0.661100105
ribosomal protein L41	RPL41	Hs.381172	-0.66066486
CD44 antigen (homing function and Indian blood group system)	CD44	Hs.306278	-0.657206608
small nuclear ribonucleoprotein polypeptide C	SNRPC	Hs.1063	-0.648570115
high-mobility group nucleosomal binding domain 2	HMGN2	Hs.181163	-0.642845036
nephronophthisis 3 (adolescent)	NPHP3	Hs.23100	-0.639861334
methionyl aminopeptidase 1	METAP1	Hs.82007	-0.63468131
serine (or cysteine) proteinase inhibitor, clade A (alpha-1 antiproteinase, antitrypsin), member 7	SERPINA7	Hs.76838	-0.625138299
retinoid X receptor, beta	RXRB	Hs.388034	-0.624620352
SLIT-ROBO Rho GTPase activating protein 1	SRGAP1	Hs.408259	-0.614551619
myelin transcription factor 1	MYT1	Hs.279562	-0.614129438
ribosomal protein S13	RPS13	Hs.446588	-0.611359806
FtsJ homolog 2 (E. coli)	FTSJ2	Hs.279877	-0.60923262
myosin, light polypeptide 6, alkali, smooth muscle and non-muscle	MYL6	Hs.77385	-0.590262904
phosphoribosylaminoimidazole carboxylase, phosphoribosylaminoimidazole succinocarboxamide synthetase	PAICS	Hs.444439	-0.589491267

involved in transcription [such as YY1 (YY1 transcription factor) - an ubiquitously distributed transcription factor implicating histone modification - TRIM29 (tripartite motif-containing 29) - involved in nucleic acid binding, and HNRPD (heterogeneous nuclear ribonucleoprotein D) that is associated with pre-mRNAs in the nucleus and appears to influence pre-mRNA processing], inflammatory response [like ITGAL (integrin lymphocyte function-associated antigen-1), which plays a central role in leukocyte intercellular adhesion - IL1RAP (interleukin 1 receptor accessory protein) – and PTPRC (protein tyrosine phosphatase receptor type C) - an essential regulator of T- and B-cell antigen receptor signaling-] and antioxidant protection elements [like PRDX5 (peroxiredoxin 5) that reduces hydrogen peroxide and alkyl hydroperoxides] (Table III).

Relevant underexpressed genes in RC encode for differentiation factors [like BMP1 (bone morphogenetic protein 1) - that induces formation of cartilage *in vivo* –, TGFB2 (transforming growth factor beta 1) – that has a role in the regulation of cartilage hypertrophic differentiation prior to development of endochondral bones – and JAG2 (jagged 2) – a ligand that actives the Notch signaling pathway, that is an intercellular

Table III. *A) 39 up-regulated genes with known function selected from 81 clones obtained by microarray analysis from MG63 cultured with RC vs MG63 cultured with WC.*

Name	Symbol	UGCluster	Score(d)
platelet-activating factor acetylhydrolase, isoform Ib, alpha subunit 45kDa	PAFAH1B1	Hs.77318	3,760802434
ribosomal protein, large P2	RPLP2	Hs.437594	3,598916023
poly(rC) binding protein 1	PCBP1	Hs.2853	3,138731546
chromosome 22 open reading frame 3	C22orf3	Hs.106730	3,108748741
protein tyrosine phosphatase, receptor type, C	PTPRC	Hs.444324	3,041177237
peroxiredoxin 5	PRDX5	Hs.31731	2,759833596
YY1 transcription factor	YY1	Hs.388927	2,539417234
Cytochrome c oxidase subunit IV isoform 1	COX4I1	Hs.433419	2,531155074
Mitogen-activated protein kinase kinase kinase 4	MAP3K4	Hs.390428	2,452636244
Cortactin binding protein 2	CORTBP2	Hs.293539	2,443621184
Component of oligomeric golgi complex 7	COG7	Hs.185807	2,320121496
Ribosomal protein S23	RPS23	Hs.386384	2,271814468
EF hand calcium binding protein 2	EFCBP2	Hs.140950	2,256694935
nucleobindin 1	NUCB1	Hs.172609	2,247353724
integrin, alpha L (antigen CD11A (p180), lymphocyte function-associated antigen 1; alpha polypeptide)	ITGAL	Hs.174103	2,235281659
filamin-binding LIM protein-1	FBLP-1	Hs.8728	2,222265509
zinc finger protein 193	ZNF193	Hs.100921	2,21549215
ciliary neurotrophic factor receptor	CNTFR	Hs.194774	2,198663898
interleukin 1 receptor accessory protein	IL1RAP	Hs.143527	2,167015819
SEC6-like 1	SEC6L1	Hs.448580	2,137135118
chromosome 20 open reading frame 17	C20orf17	Hs.150825	2,123285027
ADP-ribosylation factor 1	ARF1	Hs.286221	2,087192644
apoptosis inhibitor 5	API5	Hs.444340	2,081350007
tRNA splicing 2' phosphotransferase 1	MGC11134	Hs.326586	2,076856616
glyceraldehyde-3-phosphate dehydrogenase	GAPD	Hs.169476	2,068301757
pregnancy specific beta-1-glycoprotein 3	PSG3	Hs.438687	2,061095226
tripartite motif-containing 29	TRIM29	Hs.82237	2,049981203
flavin containing monooxygenase 1	FMO1	Hs.1424	2,040497513
paired immunoglobin-like type 2 receptor beta	PILRB	Hs.349256	1,957065758
ocular development-associated gene	ODAG	Hs.21145	1,928955239
ras homolog gene family, member C	RHOC	Hs.179735	1,923683256
up-regulated in liver cancer 1	UPLC1	Hs.437379	1,907662201
small nuclear ribonucleoprotein polypeptide C	SNRPC	Hs.1063	1,893243355
splicing factor YT521-B	YT521	Hs.86405	1,853533101
v-Ha-ras Harvey rat sarcoma viral oncogene homolog	HRAS	Hs.37003	1,846567651
rhodopsin (opsin 2, rod pigment) (retinitis pigmentosa 4, autosomal dominant)	RHO	Hs.247565	1,842494288
chromosome 9 open reading frame 60	C9orf60	Hs.29285	1,823898537
collapsin response mediator protein 1	Crmp1	Mm.290995	1,817687394
heterogeneous nuclear ribonucleoprotein D	HNRPD	Hs.438726	1,813798714

B) 45 down-regulated genes with known function selected from 73 clones obtained by microarray analysis from MG63 cultured with RC vs MG63 cultured with WC.

Name	Symbol	UGCluster	Score(d)
methyl-CpG binding domain protein 5	MBD5	Hs.458312	-3,873093825
chromosome 10 open reading frame 69	C10orf69	Hs.285818	-3,818950999
chromosome 5 open reading frame 6	C5orf6	Hs.54056	-3,63652174
transforming growth factor, beta 2	TGFB2	Hs.169300	-3,459152242
growth factor receptor-bound protein 10	GRB10	Hs.512118	-2,829770435
splicing factor 3b, subunit 4, 49kDa	SF3B4	Hs.406186	-2,77809617
thyroid hormone receptor interactor 10	TRIP10	Hs.445226	-2,741470819
guanine nucleotide binding protein (G protein), alpha 13	GNA13	Hs.9691	-2,723076805
aldehyde dehydrogenase 8 family, member A1	ALDH8A1	Hs.18443	-2,649696558
MYST histone acetyltransferase (monocytic leukemia) 3	MYST3	Hs.93231	-2,62483666
SMC4 structural maintenance of chromosomes 4-like 1 (yeast)	SMC4L1	Hs.50758	-2,611856922
AHA1, activator of heat shock 90kDa protein ATPase homolog 2 (yeast)	AHSA2	Hs.122440	-2,611550295
ubiquitin-conjugating enzyme E2N (UBC13 homolog, yeast)	UBE2N	Hs.458359	-2,543194263
RE1-silencing transcription factor	REST	Hs.401145	-2,531370308
cytoskeleton-associated protein 4	CKAP4	Hs.74368	-2,523265808
plastin 3 (T isoform)	PLS3	Hs.430166	-2,486756177
eukaryotic translation termination factor 1	ETF1	Hs.77324	-2,467830926
NFKB inhibitor interacting Ras-like 2	NKIRAS2	Hs.502910	-2,438534603
solute carrier family 2 (facilitated glucose transporter), member 1	SLC2A1	Hs.169902	-2,434571105
branched chain aminotransferase 1, cytosolic	BCAT1	Hs.438993	-2,371740726
steroid sulfatase (microsomal), arylsulfatase C, isozyme S	STS	Hs.79876	-2,312936339
titin	TTN	Hs.434384	-2,291260188
ubiquitin-conjugating enzyme E2B (RAD6 homolog)	UBE2B	Hs.385986	-2,278029746
SNAP-associated protein	SNAPAP	Hs.32018	-2,247792631
cytochrome c oxidase subunit 8A	COX8A	Hs.433901	-2,245956826
bone morphogenetic protein 1	BMP1	Hs.1274	-2,226899767
zinc finger protein 84 (HPF2)	ZNF84	Hs.22664	-2,21810777
transmembrane 4 superfamily member 9	TM4SF9	Hs.8037	-2,21299773
DEAD (Asp-Glu-Ala-Asp) box polypeptide 46	DDX46	Hs.486709	-2,153826785
vesicle transport through interaction with t-SNAREs homolog 1B (yeast)	VTI1B	Hs.419995	-2,150839463
collagen, type III, alpha 1 (Ehlers-Danlos syndrome type IV, autosomal dominant)	COL3A1	Hs.443625	-2,142999689
protein tyrosine phosphatase, non-receptor type 11 (Noonan syndrome 1)	PTPN11	Hs.83572	-2,116228766

olfactomedin 1	OLFM1	Hs.74376	-2,010601198
jagged 2	JAG2	Hs.433445	-1,988574283
protein inhibitor of activated STAT, 1	PIAS1	Hs.75251	-1,973578313
golgi autoantigen, golgin subfamily a, 1	GOLGA1	Hs.101916	-1,958436179
LATS, large tumor suppressor, homolog 1 (Drosophila)	LATS1	Hs.487239	-1,950463428
RAB27B, member RAS oncogene family	RAB27B	Hs.25318	-1,948864883
Ribosomal protein L32	RPL32	Hs.265174	-1,946028512
pleckstrin homology domain containing, family G (with RhoGef domain) member 1	PLEKHG1	Hs.51965	-1,92281589
zinc finger protein 183 (RING finger, C3HC4 type)	ZNF183	Hs.74823	-1,907827044
mitochondrial translational initiation factor 2	MTIF2	Hs.149894	-1,907521781

Table IV. *5 down-regulated genes with known function selected among 15 clones detected with microarray analysis in MG63 cultured with RCP+WCP vs MG63 cultured with RC+WC.*

Name	Symbol	UGCluster	Score(d)
ferritin, light polypeptide	FTL	Hs.433670	-1,02843608
ribosomal protein L22	RPL22	Hs.326249	-0,806781751
beta-2-microglobulin	B2M	Hs.48516	-0,774648227
solute carrier family 29 (nucleoside transporters), member 1	SLC29A1	Hs.25450	-0,764555766
golgi autoantigen, golgin subfamily a, 5	GOLGA5	Hs.241572	-0,752950064

signaling mechanism essential for proper embryonic development], signal transduction [like GRB10 (growth factor receptor-bound protein 10) - a growth factor receptor-binding protein that interacts with insulin receptors and insulin-like growth-factor receptors - TM4SF9 (tetraspanin 5) - a member of the transmembrane 4 superfamily – and PTPN11 (protein tyrosine phosphatase non-receptor 11) - a member of the protein tyrosine phosphatase family] and extracellular matrix components [like COL3A1 (collagen type 3 alpha 1) - a fibrillar collagen that is found in extensible connective tissues such as skin, lung, and the vascular system -].

Effect of biopolymer

No gene is up-regulated in presence of polymer. Very few genes are down-regulated and none has a major regulatory role (Table IV).

DISCUSSION

Coral is used worldwide for bone reconstruction. The favorable characteristics that make this material desirable for implantation are (i) osteoinduction, (ii) and osteoconduction. These properties have been demonstrated by *in vivo* studies with animal models and clinical trials over a twenty-year period. Also poly(2-hydroxyethylmethacrylate) [poly(HEMA)] is a widely used biomaterial. Moreover, several modifications of pHEMA either to improve mechanical properties or to elicit a better biological response has been reported. The poly(HEMA-co-MMA) is capable of promoting direct bone bonding and to trigger nucleation of calcium phosphate. Co-polymers based on HEMA were also used to produce synthetic composite bone graft substitutes. By using coral and poly(HEMA), a scaffold for bone reconstruction application has recently been synthesized. Cytological, histological and genetic analyses were performed to characterize this new alloplastic material.

Quantification of mitochondrial dehydrogenase activity by MTT assay was performed as indirect detector of cytotoxicity. As expected, the polymers

supported the proliferation and growth of cells and did not elicit any evident cytotoxic effect.

These results were confirmed by *in vivo* histological analysis on biomaterial implantations. As displayed by microscopical features of animal specimens, no foreign body reaction or inflammatory cell infiltrate was elicited by the presence of coral or by the polymer, therefore this biomaterial confirmed its high biocompatibility. Moreover, it appeared to be highly resorbable. Moreover, the histological investigation has shown that the coral plus polymer was more resorbable then coral alone. The high new biomaterial resorbability could be useful when we have to regenerate sites where implants have to be successively inserted, and we do not desire a composite, residual biomaterial-newly formed bone, at the interface with the implant surface. Moreover, all specimens showed a good percentage of newly-formed bone with a slightly better performance of RCP. The high resorbability of coral will lead instead to a complete disappearance of the material and only newly formed bone will be present at the interface. Clinically, this leads to an increased implant primary stability after their positioning.

To the best of our knowledge this is the first report that specifically addresses the question of genetic effect of coral on human osteoblast-like cells by using microarray technology.

The most notable effect of corals on MG63 is a down-regulation of several factors of inflammatory response (i.e. CSF1, BAT1, SCYE1 and LTBR). We suggest that this modulation of immunity makes coral more similar to the "self ", as confirmed in histological data where bone is closely apposed to the coral surface and no relevant inflammatory reaction is detected. Moreover, some components of extracellular matrix are modulated and they may have a role in coral osteo-conduction and osteo-induction. COL1A2, CD44 and IGF1R are down-regulated. They are functionally related to collagen I, osteopontin and insulin-like growth factor, respectively. These proteins are mediators of osteogenesis (21).

The comparison between RC and WC produces intriguing results that may explain the supposed higher osteogenic effect for RC. Meanwhile TGFB1 is a major regulator of osteogenesis and its production coincides with osteoblast migration, differentiation, and extracellular matrix production (22). TGFB2 has a role in the regulation of cartilage hypertrophic differentiation prior to the development of endochondral bones (23). RC induces a down-regulation of TGFB2 and may facilitate the direct ossification. In a similar way, while BMPs (2-7) are enhanced during osteogenesis (24, 25), BMP1 (or procollagen C proteinase) induces formation of cartilage *in vivo* (26). RC causes a down-regulation of BMP1 and may facilitate the ossification process. Finally, by using microarray technology, no relevant genetic effect of polymer was detected. It can be considered as inert material and it maintains the biological properties of corals. In conclusion, the gene expression changes observed *in vitro* may be used from a clinical perspective for implant monitoring and prediction of outcome. Indeed, the down-regulation of several factors of inflammatory response may indicate a good clinical integration, while the up-regulation of genes involved in matrix deposition and ossification may suggest a more rapid new bone formation *in vivo*. These qualities would make this new material an ideal bone graft material.

However, since an *in vitro* system differs from an *in vivo* system, our microarray data have an indicative but not absolute value, even if they were extensively used in works dealing with materials testing on cells (27, 28). Indeed, MG63 are osteoblast-like cells and not normal osteoblasts (29). Moreover, a monolayer cell stratum differs significantly from bone tissue, where osteoblasts are resident in a bone matrix. The advantages of using MG63 is related to the fact that it is a cell line and not a primary culture; in this way the reproducibility of the data is higher because there is no variability of the subject studied (30). Primary cell cultures, on the other hand, provide a source of more normal, non-malignant cells, but they also contain a heterogeneous cell population, often containing contaminating cells of different types and cells in variable differentiation states. This variability in cell type could lead to a less precise demonstration of the coral and biopolymer effects. Moreover, we chose to perform the experiment after 24 hours of stimulation in order to obtain information on the early stages of stimulation.

In conclusion, the present results show that coral and the polymer used were biocompatible both *in vitro* and *in vivo*. RC seem to have a higher

osteogenic effect that can be related to regulation of several genes, among them TGFB2 and BMP1. Indeed, microarray analysis showed that corals modulate inflammatory response and extracellular matrix components. The polymer is an inert material and it maintains the biological properties of corals.

ACKNOWLEDGEMENTS

This work was supported in whole or in part by the National Scientific Research Programme PRIN 2008 number 20087BNE3K_003; by grants from University of Ferrara, Italy (F.C.), Guya-bioscience, Ferrara, Italy (F.C.), and Fondazione CARISBO (F.P.); by the National Research Council (C.N.R.), Rome, Italy (AP); by the Ministry of Education, University and Research (M.I.U.R.), Rome, Italy (AP) and by AROD (Research Association for Dentistry and Dermatology), Chieti, Italy (AP).

REFERENCES

1. Souyris F, Pellequer C, Payrot C, Servera C. Coral, a new biomedical material. Experimental and first clinical investigations on Madreporaria. J Maxillofac Surg 1985; 13:64-9.
2. Marchac D, Sandor G. Use of coral granules in the craniofacial skeleton. J Craniofac Surg 1994; 5:213-7.
3. Yukna RA, Yukna CN. A 5-year follow-up of 16 patients treated with coralline calcium carbonate (BIOCORAL) bone replacement grafts in infrabony defects. J Clin Periodontol 1998; 25:1036-40.
4. Sandor GK, Kainulainen VT, Queiroz JO, Carmichael RP, Oikarinen KS. Preservation of ridge dimensions following grafting with coral granules of 48 post-traumatic and post-extraction dento-alveolar defects. Dent Traumatol 2003; 19:221-7.
5. Jammet P, Souyris F, Baldet P, Bonnel F, Huguet M. The effect of different porosities in coral implants: an experimental study. J Craniomaxillofac Surg 1994; 22:103-8.
6. Damien CJ, Ricci JL, Christel P, Alexander H, Patat JL. Formation of a calcium phosphate-rich layer on absorbable calcium carbonate bone graft substitutes. Calcif Tissue Int 1994; 55:151-8.
7. Pollick S, Shors EC, Holmes RE, Kraut RA. Bone formation and implant degradation of coralline porous ceramics placed in bone and ectopic sites. J Oral Maxillofac Surg 1995; 53:915-22.
8. Piattelli A, Podda G, Scarano A. Clinical and histological results in alveolar ridge enlargement using coralline calcium carbonate. Biomaterials 1997; 18:623-7.
9. Grillo MC, Goldberg WM, Allemand D. Skeleton and sclerite formation in the precious red coral Corallium rubrum. Marine Biology 1993; 117:119-28.
10. Cuif J-P, Dauphin Y, Doucet J, Salome M, Susini J. XANES mapping of organic sulfate in three scleractinian coral skeletons. Geochimica et Cosmochimica Acta 2003; 67:75-83.
11. Saini R, Bajpai J, Bajpai AK. Synthesis of poly (2-hydroxyethyl methacrylate) (PHEMA) based nanoparticles for biomedical and pharmaceutical applications. Methods Mol Biol 2012; 906:321-8.
12. Su J, Iomdina E, Tarutta E, Ward B, Song J, Wildsoet CF. Effects of poly(2-hydroxyethyl methacrylate) and poly(vinyl-pyrrolidone) hydrogel implants on myopic and normal chick sclera. Exp Eye Res 2009; 88:445-57.
13. Suhag GS, Bhatnagar A, Singh H. Poly(hydroxyethyl methacrylate)-based co-polymeric hydrogels for transdermal delivery of salbutamol sulphate. J Biomater Sci Polym Ed 2008; 19:1189-200.
14. Atzet S, Curtin S, Trinh P, Bryant S, Ratner B. Degradable poly(2-hydroxyethyl methacrylate)-co-polycaprolactone hydrogels for tissue engineering scaffolds. Biomacromolecules 2008; 9:3370-7.
15. Li X, Xu J, Filion TM, Ayers DC, Song J. pHEMA-nHA encapsulation and delivery of vancomycin and rhBMP-2 enhances its role as a bone graft substitute. Clin Orthop Relat Res 2013; 471:2540-7.
16. Santin M, Huang SJ, Iannace S, Ambrosio L, Nicolais L, Peluso G. Synthesis and characterization of a new interpenetrated poly(2-hydroxyethylmethacrylate)-gelatin composite polymer. Biomaterials 1996; 17:1459-67.
17. De Rosa M, Carteni M, Petillo O, et al. Cationic polyelectrolyte hydrogel fosters fibroblast spreading, proliferation, and extracellular matrix production: Implications for tissue engineering J Cell Physiol 2004; 198:133-43.
18. Carinci F, Piattelli A, Stabellini G, Palmieri A, Scapoli L, Laino G, Caputi S, Pezzetti F. Calcium sulfate:

analysis of MG63 osteoblast-like cell response by means of a microarray technology. J Biomed Mater Res B Appl Biomater 2004; 71:260-7.

19. Santarelli A, Lo Russo L, Bambini F, Campisi G, Lo Muzio L. New perspectives in medical approach to therapy of head and neck squamous cell carcinoma. Minerva Stomatol 2009; 58:445-52.
20. Bambini F, Santarelli A, Marzo G, Rubini C, Orsini G, Di Iorio D, Lo Russo L, Lo Muzio L. CD3 and CD20 expression in titanium vs zirconia peri-implant soft tissues: A human study. Eur J Inflamm 2013; 11:305-10.
21. Li G, Virdi AS, Ashhurst DE, Simpson AH, Triffitt JT. Tissues formed during distraction osteogenesis in the rabbit are determined by the distraction rate: localization of the cells that express the mRNAs and the distribution of types I and II collagens. Cell Biol Int 2000; 24:25-33.
22. Steinbrech DS, Mehrara BJ, Rowe NM, Dudziak ME, Luchs JS, Saadeh PB, Gittes GK, Longaker MT. Gene expression of TGF-beta, TGF-beta receptor, and extracellular matrix proteins during membranous bone healing in rats. Plast Reconstr Surg 2000; 105:2028-38.
23. Alvarez J, Sohn P, Zeng X, Doetschman T, Robbins DJ, Serra R. TGFbeta2 mediates the effects of hedgehog on hypertrophic differentiation and PTHrP expression. Development 2002; 129:1913-24.
24. Yazawa M, Kishi K, Nakajima H, Nakajima T. Expression of bone morphogenetic proteins during mandibular distraction osteogenesis in rabbits. J Oral Maxillofac Surg 2003; 61:587-92.
25. Campisi P, Hamdy RC, Lauzier D, Amako M, Rauch F, Lessard ML. Expression of bone morphogenetic proteins during mandibular distraction osteogenesis. Plast Reconstr Surg 2003; 111:201-8; discussion 9-10.
26. Tabas JA, Zasloff M, Wasmuth JJ, Emanuel BS, Altherr MR, McPherson JD, Wozney JM, Kaplan FS. Bone morphogenetic protein: chromosomal localization of human genes for BMP1, BMP2A, and BMP3. Genomics 1991; 9:283-9.
27. Bambini F, Greci L, Meme L, Santarelli A, Carinci F, Pezzetti F, Procaccini M, Lo Muzio L. Raloxifene covalently bonded to titanium implants by interfacing with (3-aminopropyl)-triethoxysilane affects osteoblast-like cell gene expression. Int J Immunopathol Pharmacol 2006; 19:905-14.
28. Bambini F, Pellecchia M, Memè L, Santarelli A, Emanuelli M, Procaccini M, Lo Muzio L. Anti-inflammatory cytokines in peri-implant soft tissues: A preliminary study on humans using cDNA microarray technology. Eur J Inflamm 2007; 5:121-27.
29. Lepore S, Milillo L, Trotta T, et al. Adhesion and growth of osteoblast-like cells on laser-engineered porous titanium surface: expression and localization of N-cadherin and beta-catenin. J Biol Regul Homeost Agent 2013; 27:531-41.
30. Lo Muzio L, Santarelli, A, Orsini G, Meme L, Mattioli-Belmonte M, De Florio I, Gatto R, Bambini F. MG63 and MC3T3-E1 osteoblastic cell lines response to raloxifene. Eur J Inflamm 2013; 11:797-804.